Available online at www.sciencedirect.com
ScienceDirect
Journal of Magnetic Resonance 186 (2007) 330–336
JMR Journal of Magnetic Resonance
www.elsevier.com/locate/jmr

Communication

Indirect detection of NMR via geometry-dependent dipolar fields, revisited

Wei Dong, C.A. Meriles *

Physics Department, City College of New York – CUNY, 138th Street and Convent Avenue, New York, NY 10031, USA

Received 17 January 2007; revised 12 February 2007
Available online 1 March 2007

Abstract

We explore the dipolar interactions between two separate nuclear spin ensembles in a mixture containing oil and water. Here we expand initial results [C.A. Meriles, W. Dong, J. Magn. Reson. 181 (2006) 331.] to the case in which both systems have the shape of flat, stacked disks. We find that—in spite of the strong inhomogeneity of the coupling dipolar field—the signal encoded in one of the components can be made approximately proportional to the magnetization in the other. This allows us to use one of these systems as a 'sensor' to indirectly reconstruct the resonance spectrum or to determine the relaxation time of the 'sample' system. In the regime in which dipolar interactions are sufficiently strong, our method can be set to scale-up weaker signals in a non-linear fashion, which, potentially, could allow one to introduce contrast or to improve detection sensitivity of less magnetized samples.

PACS: 76.60.Jx; 75.10.Hk; 76.20.+q

Keywords: Distant dipolar fields; Dipolar field microscopy

Because dipole–dipole interactions decay as the inverse cube of the internuclear distance, dipolar effects between non-neighboring nuclei are usually deemed exceedingly small and therefore unimportant in most applications. During the past decade, however, several investigations made it clear that this argument must be handled very carefully [1–9]. The reason is that in the molecular ensemble present in all NMR experiments, the number of terms in the sum of all dipolar interactions with a given spin increases with the square of the distance to this spin. Dipolar couplings effective over macroscopic distances become therefore non-negligible when the sample magnetization is not isotropic, i.e., when contributions to the dipolar field at the center of a sphere surrounding the spin of interest do not exactly cancel. In most experiments to date, this is accomplished by inducing a magnetization grating through the application of a field gradient pulse at some stage of the NMR pulse sequence. This approach has been exploited extensively by the Warren group [4–6] and by Bowtell and collaborators [7–9] to develop a number of applications for either liquid-state NMR spectroscopy or medical imaging.

The present study entails the investigation of the long-range dipolar interactions between two neighboring but separate spin ensembles, here in the form of an oil/water mixture. Unlike prior reports [6,9–12], our strategy makes use of the dipolar fields arising from the shape and relative location of each ensemble. A central goal in these studies is to control the dipolar coupling between the two spin ensembles so as to indirectly probe one of them (playing the role of an invisible sample) through its effect on the other (operating as a sensor). This manuscript completes and expands preliminary results [13] by considering an array of a different geometry in which both oil and water phases have the shape of flat, consecutive disks with the main central axis aligned to the external magnetic field. We demonstrate that the sensor signal can be made approximately proportional to the sample magnetization

* Corresponding author. Fax: +1 212 650 7948.
E-mail address: cmeriles@sci.ccny.cuny.edu (C.A. Meriles).

1090-7807/$ - see front matter © 2007 Elsevier Inc. All rights reserved.
doi:10.1016/j.jmr.2007.02.012

making it possible to indirectly determine the sample resonance spectrum or relaxation time. The result is attractive because it proves that the sensor need not be immersed within the sample but can, instead, sit on its surface. Interestingly, the strength of the dipolar coupling between these two systems is insensitive to the absolute dimensions of the array. This leads us to envision a number of extensions of this or related schemes, this time to manipulate dipolar interactions between small, mesoscale systems.

The inset in Fig. 1 shows a picture of a setup similar to that used in our investigation. The system can be modeled as two (relatively) flat, stacked disks of distilled water (colored) and oil (Fluka DC 200) with their central axes aligned to the external magnetic field. In calculating the effect of the dipolar field of one system on the other, the presence of a dominant magnetic field $\mathbf{B}_0$ makes it possible to neglect, as usual, all non-secular contributions to this field. Further, since water ('sample') and oil ('sensor') resonance frequencies differ by almost 5 ppm (1.8 kHz in our 9.4 T magnet), one can consider the combined system as heteronuclear and limit the contribution of the 'sample' dipolar field over the 'sensor' volume to the component parallel to $\mathbf{B}_0$ (assumed along the z-axis) [13]. Although obtaining a formula that describes the spatial dependence of this latter field is difficult, a numerical calculation is straightforward [14]. Close to the interface, the z-component of the dipolar field reaches a magnitude equal to $B_{\mathrm{spl}}^{\max} = 5\mu_0 M_{\mathrm{spl}}^{(0)}/(4\pi)$, where μ_0 is the vacuum magnetic permeability and $M_{\mathrm{spl}}^{(0)}$ denotes the sample equilibrium magnetization. This amplitude decays monotonously over the sensor volume (assumed equivalent to that of the sample) to reach a value approximately 30% that of its maximum on the side of the sensor disk farthest away from the sample. At room temperature in a 9.4 T magnetic field, $B_{\mathrm{spl}}^{\max}$ amounts to roughly 12 nT (0.5 Hz ^{1}H frequency).

Fig. 2 displays the Fourier transform of the signal obtained during the 'reading period' for different contact times t_c. Successive spectra exhibit a slow but clear phase evolution that can be interpreted as the slow modulation introduced in the signal (Hahn echo) due to the cumulative effect of the sample dipolar field on the sensor. Notice that in the pulse sequence of Fig. 1, field inhomogeneities or frequency offsets are cancelled through the application of π-pulses during the 'decoding' period; long-range dipolar fields, however, remain effective due to the simultaneous inversion of sample and sensor spins. No phase change was observed in the measured signal each time the sample magnetization was saturated prior to the application of the pulse sequence, therefore confirming that the presence of the sample dipolar field is crucial. The magnitude of this field as measured from the observed phase evolution amounts to 0.35 Hz, in qualitative agreement with that

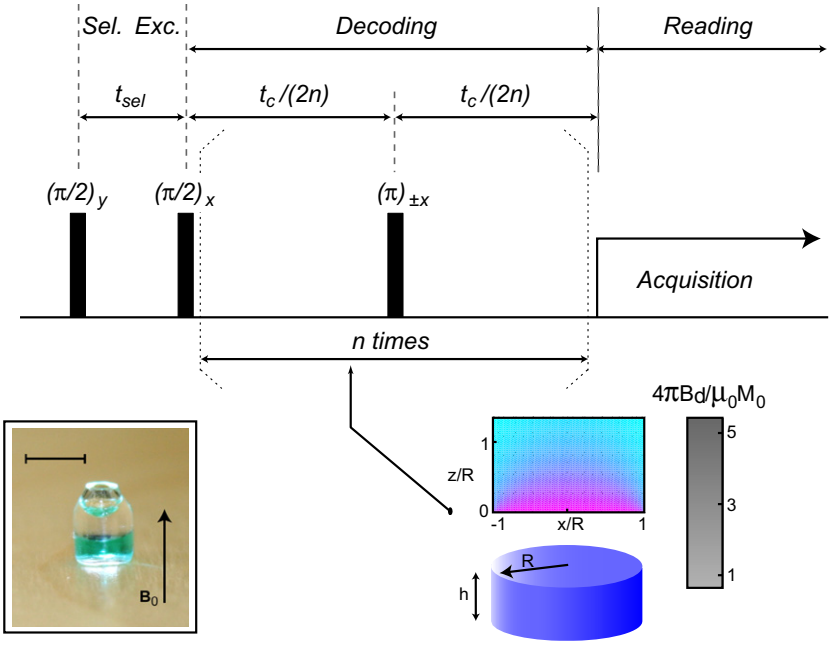

Fig. 1. *Main*: Water (sample) and oil (sensor) spin ensembles have the shape of comparable, flat disks stacked along the direction of the external static field $\mathbf{B}_0$. The pulse sequence utilized to probe the sample magnetization is shown on the top. After selective excitation, sensor spins evolve in the presence of the sample dipolar field for a variable 'contact time' t_c. Hard π-pulses of alternated phase are intercalated during this evolution to compensate for inhomogeneities of the main static field (while preserving the action of the dipolar field, see text). The echo forming after t_c is finally acquired for inspection. Throughout the sequence, t_{sel} is kept fixed at a value equal to one fourth the inverse of the frequency shift between oil and water resonances. The drawing at the right lower corner displays the dipolar field induced by the sample magnetization on the sensor volume. The calculation assumes that the sample has a height h equal to the radius R. Note that the amplitude of the dipolar field on the sensor depends only on the geometry of the sensor/sample system (and therefore remains unchanged if all dimensions in the array are simultaneously scaled). *Left lower corner:* Photograph of an array similar to that used in the experiments. Sample and sensor occupy comparable volumes and have the shape of disks of diameter approximately equal to half the height. The scale bar corresponds to 3 mm. For clarity, water at the bottom of the container was artificially colored by admixture of a green dye.

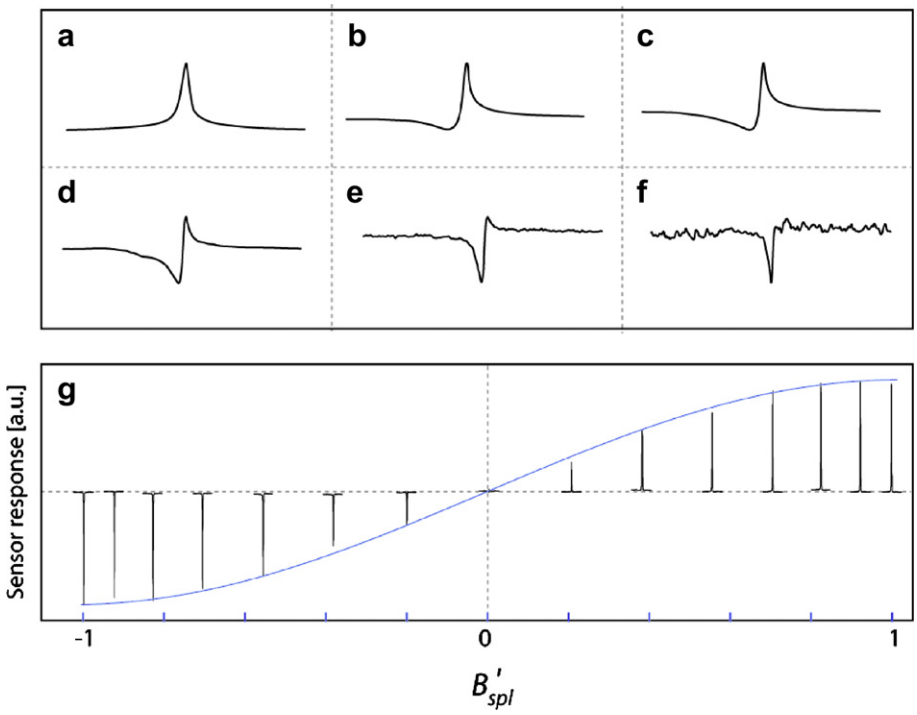

Fig. 2. Fourier transform of the sensor signal (oil) obtained after a variable contact time using the pulse sequence of Fig. 1. The sample dipolar field induces a slow precession of the sensor magnetization observable through the progressive phase change of the echo. From top to bottom, the contact time was (a) 145 ms, (b) 550 ms, (c) 750 ms, (d) 1000 ms, (e) 1250 ms, (f) 1600 ms. The average field on the sensor—approximately 0.35 Hz—is strong enough in this case to induce a 180-degree phase shift of the sensor signal. The spectral bandwidth from (a) to (c) is 2.5 kHz. (g) 'Subtraction-mode' sensor signal at $t_c = 0.8$ s as a function of the sample dipolar field. A preparation protocol similar to that of Fig. 3 was used to vary the sample magnetization and, with it, the magnitude of the relative dipolar field B'_{spl} acting on the sensor. In agreement with Eq. (3), the sensor displays a sinusoidal response of the type $S_{snr} \propto \sin(\pi B'_{spl}/2)$, here shown as a solid line for comparison.

expected from an average of the dipolar field over the sensor volume (see Fig. 1).

The effect of the sample dipolar field on the evolution of the sensor magnetization can be made more explicit by adding consecutive acquisitions while alternating both the receiver phase and initial direction of the sample magnetization [15]. In the pulse sequence of Fig. 1, the latter is accomplished by increasing in 180-degree steps the phase of the second π/2-pulse during the selective sensor excitation.[16] With this procedure, the sensor signal (after an even number of scans) becomes

$$S_{snr} \propto \int_{V_{snr}} dr^3 M^{(0)}_{snr} \sin\left(\gamma_{snr} t_c B^{(z)}_{spl}\right) \quad (1)$$

where γ_{snr} denotes the sensor gyromagnetic ratio, $B^{(z)}_{spl}$ is the (secular) dipolar field due to the sample, $M^{(0)}_{snr}$ is the equilibrium sensor magnetization and the integral is calculated over the sensor volume. Experimental results illustrating our ability to measure the sample dipolar field—and, therefore, its local magnetization—are shown in Fig. 2g for a fixed contact time t_c chosen, so that $\gamma_{snr} t_c \langle B^{(z)}_{spl}\rangle \leqslant \pi/2$ (the brackets are used to indicate average over the sensor volume). A simple protocol (similar to that of Fig. 3) was used here to scale the sample magnetization (and, therefore, the dipolar field) prior to the application of the sequence of Fig. 1. The sensor signal is observed to evolve as expected, with amplitude approximately proportional to (the sine of) the sample magnetization [17]. The response 'saturates' in the region of strongest sample dipolar field although the observed dependence can be 'relinearized' by shortening the 'decoding' time t_c (therefore forcing $\gamma_{snr} t_c \langle B^{(z)}_{spl}\rangle < \pi/2$ even in the case of maximum sample magnetization). Depending on the ratio between the contact time and the sensor relaxation time this may (or may not) result in a smaller signal amplitude (vide infra).

Dipolar couplings between the sample and sensor can be used not only to probe the sample magnetization but also to indirectly determine some of its basic NMR parameters. For example, indirect measurement of the sample T_1 via the sensor becomes straightforward with the use of a simple preparation protocol as shown in Fig. 3. Notice that diffusion and relaxation effects (of both the sample and the sensor) during the 'decoding' period remain approximately constant throughout the process and, therefore, do not hinder an accurate measurement. The same principle can be extended to indirectly determine the sample resonance spectrum. In our experiment, this is accomplished by modifying the preparation protocol of Fig. 3a to probe in a 'point-by-point' fashion the in-plane evolution of the sample magnetization after selective excitation. Fig. 3c shows the resulting evolution of the sensor signal: Fourier

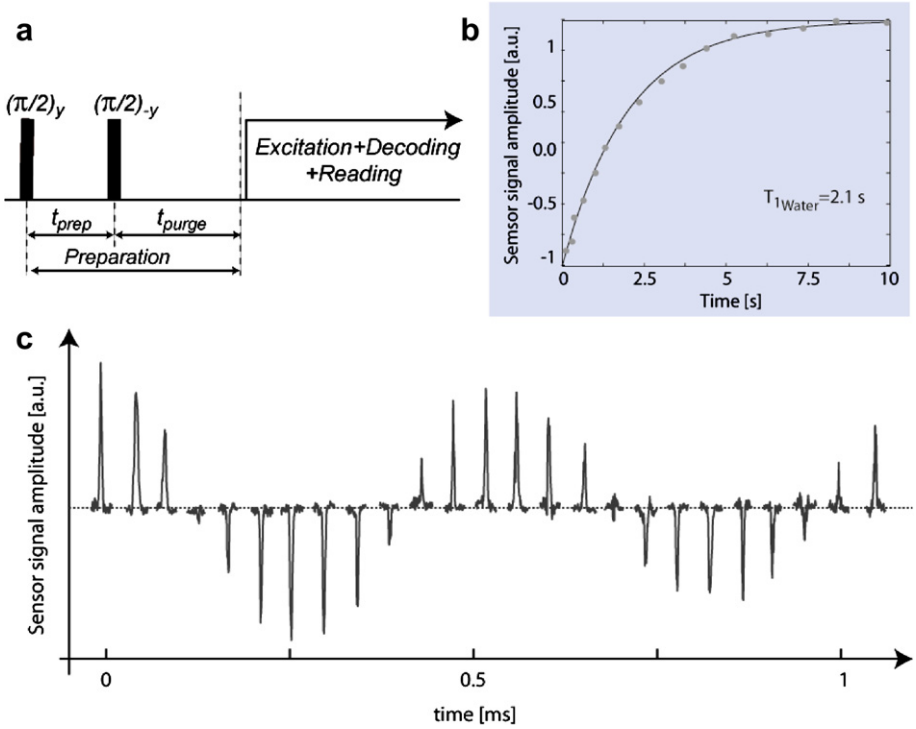

Fig. 3. (a), (b) Indirect determination of the sample relaxation time via the dipolar field on the sensor. The pulse sequence of Fig. 1 was preceded by a simple inversion-recovery protocol followed by a short purging time. Selective inversion of the sample spins was carried out by two consecutive π/2-pulses spaced by half the period corresponding to the oil-water frequency difference. The sample relaxation time was 2.1 s in good agreement with the value measured by direct observation. (c) Point-by-point determination of the sample resonance spectrum by observation of the sensor signal. A preparation protocol similar to that shown in (a) but with a variable inter-pulse spacing was applied to monitor the in-plane evolution of the sample magnetization. The contact time t_c was 0.5 s.

transform along this time axis leads to a ~1.8 kHz-shifted sample resonance peak in agreement with the measured chemical shift of the sample (water) relative to the sensor (oil) resonance frequency.

A facet of the scheme introduced here that is worth exploring in some detail is the effect of relaxation on the amplitude of the signal encoded in the sensor. Shown in Fig. 4 is the evolution of the Fourier-transformed FID as a function of the contact time t_c. As before (see Fig. 2g), subsequent acquisitions of the sensor magnetization were co-added while simultaneously alternating the detector phase and the initial orientation of the sample magnetization. For contact times much shorter than the inverse of the dipolar field (expressed in frequency units), the peak amplitude tends to zero, as expected. At later times, Eq. (3) predicts a sinusoidal growth [17] with its first maximum occurring at a time $t_c \cong (\pi/2)(\gamma_{snr}\langle B^{(z)}_{spl}\rangle)^{-1}$ (approximately 0.8 s). In practice, however, the maximum signal is observed at much shorter times (~0.2 s), when the gain arising from a greater phase change of the sensor magnetization is not overshadowed by transverse and longitudinal relaxation of both sample and sensor spins.

Qualitatively, the effect of relaxation on the signal amplitude can be taken into account by introducing a time dependence on the sensor (and sample) magnetizations. Eq. (1) then writes

$$S_{snr}(t_c) \propto \int_{V_{snr}} dr^3 M^{(0)}_{snr} \exp(-t_c/T_{snr}) \sin\left(\int_0^{t_c} dt \gamma_{snr} B^{(0)}_{spl} f(t)\right) \quad (2)$$

where T_{snr} represents the transverse relaxation time of the sensor and $f(t)$ is a function that takes into account the decay of the sample dipolar field during the 'decoding' period. This decay can be induced either by longitudinal sample relaxation or the repeated application of π-pulses affected by rf inhomogeneity. Fig. 4 shows the result for the case $f(t) = \exp(-t/T_{spl})$, with T_{spl} denoting the (effective) longitudinal relaxation time of the sample. Shown for comparison is also the curve obtained through a numerical simulation in which the sensor was modeled as an aggregate of classical spins obeying Bloch equations; both curves qualitatively reproduce the observed behavior although overall agreement (particularly at short times) is moderate. We presently ignore the causes but we speculate that this is due to susceptibility effects at the interface and/or artifacts in the selective excitation of the sensor magnetization due to modest shimming and rf homogeneity.

At long contact times, the observed behavior is dominated by the transverse relaxation rate of the sensor. In the presence of a relatively strong static field inhomogeneity such as that of our setup, spin diffusion does contribute to induce a faster decay. As expected, the inset in Fig. 4

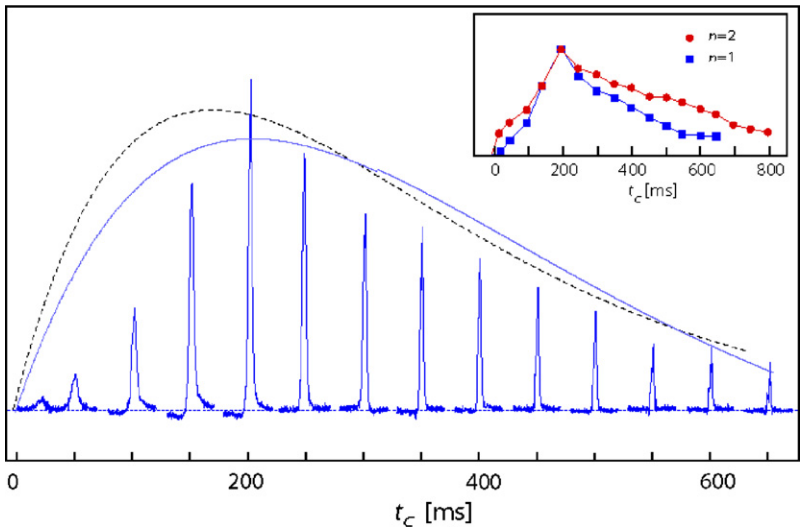

Fig. 4. Signal amplitude as a function of the contact time. In-phase spectra were obtained by pairing subsequent FID's while synchronously alternating the sign of the initial sample magnetization (see text). After a rapid initial growth, the amplitude diminishes exponentially. The dashed curve corresponds to Eq. (2) with $f(t) = \exp(-t/T_{spl})$ whereas the continuous curve indicates the result of a numerical simulation. Only one inversion pulse was applied during t_c. *Inset:* Decay of the signal due to diffusion can be mitigated by incrementing the number of inversion pulses. Shown for comparison are the results using one and two inversion pulses during t_c.

shows that this effect can be partly mitigated by increasing the number of inversion pulses (until the cumulative action of rf inhomogeneity on the sample dipolar field precludes further improvement [18]). We will soon make use of this feature to explore different scenarios in which the ratio between the contact time t_c and the sensor decoherence time T_{snr} is varied.

Assuming that the sensor has been chosen to provide the best possible signal-to-noise ratio, Eq. (2) indicates that our ability to boost detection sensitivity of the sample signal depends critically on the product of the time $t_c^{opt} \approx \pi/2(\gamma_{snr}\langle B_{spl}^{(z)}\rangle)^{-1}$ (necessary to induce maximum modulation of the sensor magnetization) and its transverse relaxation rate $(T_{snr})^{-1}$: full sensor sensitivity will be attainable when $t_c^{opt}/T_{snr} \approx 0.3$ or smaller but will be correspondingly reduced in other cases [19]. For instance, in Fig. 4 the highest signal amplitude at ~200 ms amounts to only a small fraction (~10%) of the theoretical maximum (which, in the absence of relaxation, corresponds to the 'full' water signal [20] and occurs at the 'optimum' contact time $t_c^{opt} \sim 0.8$s). Although indirect detection of the sample signal as shown here becomes obviously impractical in the presented setting, the use of the sensor may be favored in situations where stronger dipolar couplings make the contact time significantly shorter or when detection sensitivity in the sensor largely surpasses that possible in the sample [13,21]. Note that in this latter scenario, a contact time much shorter than the 'optimum' value may still make indirect detection comparatively favorable.

A regime in which the contact time is much shorter than the spin decoherence time can be exploited so as to determine the sample magnetization via the time needed to induce in the sensor a predetermined phase change (as opposed to detecting the phase evolution over a fixed contact time). In this 'inverse' mode, the contact time required in a sample with half the magnetization would last approximately twice as long but the overall phase change in the sensor signal would remain unaltered. The advantage is that, under the right conditions, a weaker sample magnetization can be probed almost without compromising detection sensitivity. To render this idea more formal, we write

$$t_c = \frac{\phi}{\gamma_{snr}\left\langle B_{spl}^{(z)}\right\rangle}, \tag{3}$$

indicating that for every local dipolar field $\langle B_{spl}^{(z)}\rangle$ the contact time t_c is chosen so as to induce in the sensor a phase change ϕ ($\leqslant\pi/2$). If, for simplicity, we assume [19] $T_{snr} \ll T_{spl}$, we use Eq. (2) (with $f(t) = 1$) to write

$$S_{snr}\left(B'_{spl}\right) \propto M_{snr}^{(0)} \sin\phi \exp\left(-\frac{t_c^{ref}}{T_{snr}B'_{spl}}\right). \tag{4}$$

Here $B'_{spl} = \langle B_{spl}^{(z)}\rangle/\langle B_{ref}^{(z)}\rangle$ represents the local magnetic field relative to that in a reference (which could be a sample or section of the sample with a strong magnetization) and t_c^{ref} indicates the time needed to induce in the latter a phase change ϕ. (Fig. 5) displays the normalized sensor signal $S'_{snr} = S_{snr}(B'_{spl})/S_{snr}(1)$ as a function of the relative, local dipolar field for different values of t_c^{ref} and T_{snr}; in this drawing the diagonal corresponds to the usual, inductive detection where the signal-to-noise ratio scales linearly with the amplitude of the sample magnetization. As long as the contact time remains shorter than the sensor (and sample) relaxation times, the curves indicate a slower loss of sensitivity relative to that typical in standard detection methods. In our experiment, we reach this regime by choosing $t_c^{ref} = 300$ ms ($\phi \sim \pi/5$) and by applying a total of six π-pulses during the contact time (which allows us to increase

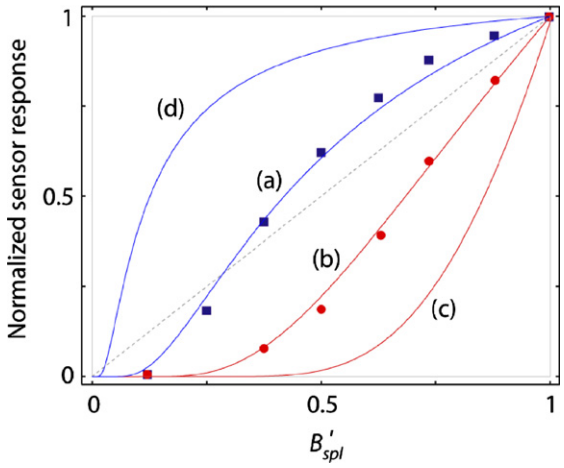

Fig. 5. The magnetization of the sample (as compared to that of a reference) can be determined via the time needed to induce a predetermined phase shift of the sensor spins. The graph shows the normalized sensor signal as a function of the relative sample magnetization B'_{spl} (Eq. (4), see text) for a sensor operated in this modality. The (dashed) diagonal indicates a 'linear' response; 'amplification' of the signal due to weaker sample magnetization is possible when the reference contact time is shorter than the sensor relaxation time T_{snr} (and T_{spl}). (a) With a reference contact time of only 300 ms ($\phi = \pi/5$), this regime can be reached by using six inversion pulses during t_c. Squares indicate experimental points; the solid line corresponds to Eq. (4) with $t_c^{ref} = 300$ ms and $T_{snr} = 600$ ms. (b) The opposite scenario takes place when the number of inversion pulses is reduced to only one. Experimental data (circles) and solid line ($t_c^{ref} = 300$ ms and $T_{snr} = 200$ ms in Eq. (4) show reasonable agreement. (c) Calculated response for the case $t_c^{ref} = 800$ ms and $T_{snr} = 200$ ms corresponding to $\phi = \pi/2$. (d) Eq. (4) with $\phi = \pi/2$ and $t_c^{ref}/T_{snr} = 0.1$.

T_{snr} to ~700 ms). This strategy fails when a longer t_c^{ref} (i.e., a greater phase change ϕ) is necessary to increase the absolute signal amplitude (see Eq. (4)) or when the interpulse spacing in the CPMG train is long (resulting in a shorter T_{snr}).

In summary, this manuscript has explored the dipolar interactions between two separate, macroscopic nuclear spin ensembles having the shape of stacked, collinear cylinders. We find that the sensor signal roughly scales with the local sample magnetization thus making it possible to indirectly determine the resonance spectrum or relaxation rate in one of them via its effect on the other. When the decoherence time of the sensor magnetization is sufficiently long (or when the sample/sensor dipolar coupling is sufficiently strong), our strategy can be altered to increase detection sensitivity only at the expense of extending the contact time. In an array where the sensor is free to move over the surface of a larger, extended sample, this scheme could be used to advantage to explore areas of the sample that are weakly magnetized or as a way to introduce (image) contrast [22]. It is worth stressing at last that the strength of the coupling between the spin ensembles depends only on the magnetization and relative geometry, which makes this strategy appealing as the absolute dimensions of the components diminish. Possibly the most exciting extension of these ideas entails the control of dipolar interactions in solids. At the low temperatures required for this implementation, high-sensitivity detection methods could be exploited to indirectly probe the sample magnetization with a spatial resolution defined by the size of the sensor [21]. Work along these lines is currently under way in our laboratory.

Acknowledgments

The authors are indebted to Dr. Boris Itin for valuable assistance with some of the experiments reported here. This research was supported by NSF through a CAREER program. W.D. and C.A.M. are members of the New York Structural Biology Center (NYSBC), a STAR center supported by the New York State Office of Science, Technology and Academic Research. NMR resources at the NYSBC are supported in part by the National Institutes of Health (Grant P41 GM66354).

References

[1] G. Deville, M. Bernier, J.M. Delrieux, NMR multiple echoes observed in solid ^{3}He, Phys. Rev. B 19 (1979) 5666.
[2] A. Vlassenbroek, J. Jeener, P. Broekaert, Macroscopic and microscopic fields in high-resolution liquid NMR, J. Magn. Reson. Ser. A 118 (1996) 234.
[3] M.H. Levitt, Demagnetization field effects in two-dimensional solution NMR, Concepts Magn. Reson. 8 (1996) 77.
[4] W.S. Warren, W. Richter, A.H. Andreotti, B.T. Farmer, Generation of impossible cross peaks between bulk water and biomolecules in solution NMR, Science 262 (1993) 2005.
[5] S. Vathyam, S. Lee, W.S. Warren, Homogeneous NMR spectra in inhomogeneous fields, Science 272 (1996) 92.
[6] W. Richter, S. Lee, W.S. Warren, Q. He, Imaging with intermolecular zero-quantum coherences in solution nuclear magnetic resonance, Science 267 (1995) 654.
[7] R. Bowtell, R.M. Bowley, P. Glover, Multiple spin echoes in liquids in a high magnetic field, J. Magn. Reson. 88 (1990) 643.
[8] R. Bowtell, Indirect detection via the dipolar demagnetizing field, J. Magn. Reson. 100 (1992) 1.
[9] R. Bowtell, S. Gutteridge, C. Ramanathan, Imaging the long-range dipolar field in structural liquid state samples, J. Magn. Reson. 150 (2001) 147.
[10] J. Granwehr, J.T. Urban, A.H. Trabesinger, A. Pines, NMR detection using laser-polarized xenon as a dipolar sensor, J. Magn. Reson. 176 (2005) 125.
[11] S.M. Brown, P.N. Sen, D.G. Cory, Scaling Laws in NMR scattering via dipolar fields, J. Magn. Reson. 154 (2002) 154.
[12] S.M. Brown, P.N. Sen, D.G. Cory, Nuclear magnetic resonance scattering across interfaces via the dipolar demagnetizing field, J. Chem. Phys. 116 (2002) 295.
[13] C.A. Meriles, W. Dong, Indirect detection of Nuclear Magnetic Resonance via geometrically-induced long-range dipolar fields, J. Magn. Reson. 181 (2006) 331.
[14] Because the sample magnetic field is to be calculated only on the region occupied by the sensor, it is enough to divide the sample volume into sufficiently small compartments dV with magnetic moment $d\boldsymbol{\mu} = \boldsymbol{M}dV$, with $\boldsymbol{M}$ the magnetization of the sample (assumed homogeneous). The magnetic field at a given point on the sensor is obtained by co-adding the contributions to the field at a given point from all elementary dipoles $d\boldsymbol{\mu}$. See, for example, J.D. Jackson, Classical Electrodynamics, third ed., Wiley, New York, 1999, Chapter 5.
[15] Note that in the absence of dipolar fields on the sensor, this procedure exactly cancels the observed signal. See Ref. [13] for further details.

[16] This procedure also eliminates contributions due to homonuclear dipolar fields on the sensor itself. It is worth indicating, however, that homonuclear contributions are expected to be comparatively weak anyhow. This is because the longitudinal component of the sensor magnetization remains small during most of the 'decoding' period; effects due to corotating components can also be neglected given the much stronger field inhomogeneity in our setup (the line broadening of both sensor and sample resonances was ~150 Hz).

[17] A description in which the observed signal is proportional to the sine of the average phase gained by sensor spins during the contact time t_c, is strictly inconsistent with formula (1). Yet, when $t_c < \pi/2(\gamma_{snr}\langle B_{spl}^{(z)}\rangle)^{-1}$, this simpler representation is approximately correct as a simple numerical calculation demonstrates for the system under consideration.

[18] In our setup, this was observed after 15 inversions.

[19] The reader is reminded that T_{snr} is the *transverse* relaxation time of the sensor whereas T_{spl} indicates the longitudinal relaxation time of the sample. Therefore, $T_{snr} \ll T_{spl}$ will be the most common scenario.

[20] Inhomogeneity of the sample dipolar field over the sensor contributes to further reduce the amplitude of the sensor signal. In the absence of relaxation and for a cylindrical sensor of height equal to its radius, the maximum encoded signal corresponds to approximately 30% of that induced by the sensor full magnetization.

[21] C.A. Meriles, Optical detection of nuclear magnetic resonance at the sub-micron scale, J. Magn. Reson. 176 (2005) 207.

[22] Note that in this case, an 'encoding' period is necessary to select the part of the sample to be probed. See Refs. [13] and [21] for further details.